DUPLICATE

# Forecasting Research

Forecasting Research Division
Technical Report No. 84

## Tests of the proposed semi-Lagrangian Advection scheme Part 1: Passive advection of a scalar.

by
Mark H. Mawson

February 1994

Meteorological Office
London Road
Bracknell
Berkshire
RG12 2SZ
United Kingdom

ORGS UKMO F
National Meteorological Library
FitzRoy Road, Exeter, Devon. EX1 3PB

Forecasting Research Technical Note No. 84

# Tests of the proposed semi-Lagrangian Advection scheme. Part 1: Passive advection of a scalar.

Mark H. Mawson

February 1994

This document has not been published. Permission to quote from it must be obtained from the director of Forecasting Research.

## Abstract

The proposed semi-Lagrangian advection scheme for the Unified Model is evaluated by considering passive advection of a scalar on the sphere. The scheme consists of two main parts: a routine to calculate the departure point of the trajectory, and a routine to interpolate the data to this point. The departure point step was tested in isolation and it is shown that it may be inappropriate to use this particular choice of departure point scheme in low resolution models. The interpolation routines are discussed and some suggestions about alternatives which should be investigated at a later date are made. The interpolation step in the proposed scheme can be made both monotone and conservative. The effects of doing this are demonstrated in the test problems.

# 1 The passive advection problem.

The passive advection problem in its Lagrangian form is simply

$$\frac{DS}{Dt} = 0 \tag{1.1}$$

where $S$ is some scalar quantity and the wind field is given for the domain and time interval we are interested in. This is a problem which can be considered as trivial since most solutions are obvious and could easily be done without resort to complicated numerical algorithms. However, if we do resort to such numerical techniques we find that they find this a serious problem, and this allows us an easy way to both verify that the codes are working correctly and to compare schemes against each other. We wish to solve the problem on a grid which is equally spaced in latitude/longitude and defined in some given way in the vertical. The spacing in the latitudinal direction does not have to be equal to the spacing in the longitudinal direction. Ideally we would like to solve this equation in its Lagrangian form, but this is not possible if we wish to impose this grid-structure at all times. This leaves us with two approaches, the Eulerian method and the semi-Lagrangian method. The Eulerian approach is to re-write equation (1.1) in its Eulerian form, which for the sphere is

$$\frac{\partial S}{\partial t} + \frac{u}{rcos\phi}\frac{\partial S}{\partial \lambda} + \frac{v}{r}\frac{\partial S}{\partial \phi} + w\frac{\partial S}{\partial r} = 0 \tag{1.2}$$

where $(\lambda, \phi, r)$ are spherical polar co-ordinates. We can then solve this equation by a suitable finite-difference method. This is the approach currently used in the Unified Model. The semi-Lagrangian approach is to assume that the points on the grid are the arrival points of Lagrangian trajectories. To calculate the solution of equation (1.1) we need to find the departure points for these trajectories and then interpolate the data to find the value at the starting point. Thus a semi-Lagrangian scheme is naturally made up of two components, a departure point calculation, and an interpolation scheme. For a review of semi-Lagrangian meth-

ods see Staniforth [11]. In this report we discuss the proposed semi-Lagrangian scheme for the Unified Model as described in Mawson [8] with respect to a scalar. We test the scheme on some standard problems which involve solid body rotation of a given shape. These test problems do not test the vertical part of the trajectory code, nor the vertical part of the interpolation code, except trivially. These parts of the routines can be easily checked using simple analytic data.

## 2 Departure Point Calculation.

The proposal is to use the scheme of McGregor [5] rather than that of Robert [10] which has been the basis of other centres' semi-Lagrangian models. This is because in principle it is computationally cheaper and just as accurate. It is envisaged that Robert's scheme will be available as an option at a later date. The basic idea of McGregor's scheme is to expand the departure point as a Taylor series in time to obtain,

$$P(t_0) = P(t_0 + \Delta t) + \sum_{n=1}^{\infty} \frac{(-\Delta t)^n}{n!} \frac{D^n P(t_0 + \Delta t)}{Dt^n} \tag{2.3}$$

We can calculate this to as many or as few terms as we desire provided that we can evaluate the time derivative on the right-hand-side of the equation. McGregor does this by approximating the time derivative by its Eulerian form, as per equation (1.2), and ignoring the local time derivative that appears in the Eulerian expansion. This procedure is performed using a Cartesian co-ordinate system to represent the co-ordinates of the position vector $P$. The full scheme is thus,

1. Transform position vector from spherical polar co-ordinates to cartesian co-ordinates.

2. Calculate the Taylor series to order N.

3. Transform back to spherical polar co-ordinates.

Since the Cartesian co-ordinates of $P$ are independent we can calculate the three components simultaneously. As shown in McGregor [5] the first term of the Taylor series can be found analytically and we only require a numerical form of equation (1.2) for terms greater than one. The finite difference form used is

$$\frac{1}{rcos\phi}\overline{\overline{u}^{r}\delta_{\lambda}X}^{\lambda}+\frac{1}{r}\overline{\overline{v}^{r}\delta_{\phi}X}^{\phi}+w\delta_{2r}X \tag{2.4}$$

where a C grid Charney-Phillips data staggering has been assumed. At the top most level the vertical averages of $u$ and $v$ are set to the values of $u$ and $v$ at the level below. The equation at the pole is given by simply meaning the finite difference form of the equation.

The code was tested on various size grids with a Courant number $\nu = 1$ so that if the wind field was purely zonal, v=w=0, then exactly one grid-length should be moved in a timestep. Table 2.1 shows the results for $N = 4$ at the equator for various numbers of points in the $\lambda$ direction for purely zonal flow with $\nu = 1$ and at a radius of 6378750 metres. The table shows the fraction of the grid-length moved in the $\lambda$ direction, ideally 1, and also the error that occurs in the local vertical. No errors occur in the $\phi$ direction.

As can be seen the results are very good for the departure point distance in the horizontal, however the errors in the vertical are unacceptably large. The reason for this can be found by finding the analytic solution after taking just 1 term of the Taylor expansion. The value of the height returned after one term of the expansion is

$$R\sqrt{(1+(\nu*\Delta\lambda)^2)}$$

where $R$ is the height that the solution should have. The error is reduced as more terms are taken in the expansion, but for low resolutions the number of terms required will be large and this scheme will cease to be cheaper than the method of Ritchie, which does not suffer from this problem. The same test was run with

| Points | Fraction of grid-length moved | Height Error (m) |
|---|---|---|
| 16 | 0.99917 | 12235 |
| 48 | 0.99997 | 155 |
| 72 | 0.99998 | 31 |
| 96 | 0.99999 | 10 |
| 288 | 0.99999 | 1 |

Table 2.1:

288 points and a constant value of $u = 150ms^{-1}$ which is typical of the maximum value found in the operational forecast model. For this problem the error was of the order $10m$ which is probably insignificant at the levels where this value is found. However this error will probably be systematic and so may be relevant, this should be investigated in more detail with real data.

# 3 Interpolation scheme.

## 3.1 Order of Interpolation.

The consensus of opinion is that the interpolation scheme in a semi-Lagrangian model should be at least a cubic. Some authors have advocated even higher order, for example Leslie and Purser [6] used quintic interpolation. The choice of which form of cubic is open to some debate. Williamson and Rasch [12] compared several forms of Hermite cubic for shape-preserving algorithms. The Hermite cubic in one direction can be made monotone be simply modifying the derivatives. It is noted that if no modifications are made to the basic Hermite cubic, then it is identical to the Lagrange cubic. Bermejo and Staniforth [2] found that for their monotone scheme, and also for their non-monotone scheme, cubic splines performed better than cubic Lagrange. The semi-Lagrangian scheme for the Unified

Model will allow a choice of cubic, and possibly higher order interpolants, via a simple switch which can be set via a *user interface*. The first scheme coded, and in use in these tests, is the cubic Lagrange interpolant.

The next issue is how to implement the chosen cubic. For Lagrange interpolation in a particular direction we need four data points to obtain a cubic. If we wish to interpolate to points between the value at the edge of our domain and the point one grid-length in then we are left with a choice of how to do this. This is because to choose four points centred about this location will require us to go outside the domain, which is not possible. The choice is either to use a linear interpolant at such points, or to use cubic interpolation and not centre the cubic about the point we wish to interpolate to. At the moment we have chosen to use the linear interpolant, the other choice should be investigated at a later date. To evaluate the cubic interpolant in three-dimensions requires a total of 21 one-dimensional cubic interpolants. This is a large cost and some people, for example Bates, use a cheaper version which requires only 11 1-D cubic interpolants and 4 1-D linear interpolants. They replace the cubic interpolation required at the end points of the last 1-D cubic to be done with a linear interpolant. For the moment we have coded the full 21 1-D version, the cheaper option will be added later.

The final issue, and one which has been ignored in the literature so far, is what order should we do these 1-D interpolants in ? So far they have been implemented in the order, y, x, z. This has the advantage of doing the horizontal interpolations along co-ordinate surfaces and is thus cheaper and easier to implement than would be the ordering, z,y,x. This is because if we interpolate in the vertical first we may find that some of the points we require to perform the horizontal interpolation lie below the lowest level of data. This can easily be seen to be true if you draw a simple picture of sloping co-ordinate surfaces near the ground. The question

is thus, does the order really matter ? This is another area where we need to do some work, particularly with the proposed semi-implicit integration scheme for the Unified Model evaluating many of its horizontal derivatives along constant z surfaces with the intention of obtaining better solutions. If this premise is true, then it suggests that better solutions may also be obtained from the ordering z,y,x. At the moment the cubic Lagrange scheme as coded is in the order y,x,z.

## 3.2 Monotonicity and Conservation.

There are two basic approaches to obtain monotonicity. The first is to choose an interpolant that is guaranteed to be monotone. The second is to use any interpolant, but then to constrain the answer given by it to remain within the values of the data at the grid-points which surround it. The first approach is very hard to implement and will be disregarded. The second method was looked at recently by Bermejo and Staniforth [2]. Priestley [9] then showed that it was possibly to extend this idea a little and obtain a method which could also be conservative and monotone. The major criticism levelled at the semi-Lagrangian method has been its non-conservation of the global integral of the quantity being advected, something that is easy to enforce in Eulerian models. His idea was to first take a high order interpolated solution and make it monotone, similarly to Bermejo and Staniforth. Then to calculate a lower order monotone solution to the same problem. He then seeks to find a conservative solution which lies between these high-order and low-order solutions. Since both solutions are monotone, so is the conservative one. The only problem is that a conservative solution cannot be guaranteed to exist. This can be due to the high-order and low-order solutions being very similar, so there is little scope for regaining conservation. For problems such as the cosine bell considered in the next section conservation is impossible to enforce most of the time. This is because the monotone solutions contain less

of the quantity than was around at the start of the timestep and the montonicity constraint stops us adding back any more. For general data the amount of leeway between the high order and low order solutions has been found to be sufficient for shallow-water test problems, see Garcia-Navarro and Priestley [3] and Gravel and Staniforth [4].

We have implemented the method of Priestley [9] and at the moment the only monotone low-order scheme available is linear Lagrange interpolation, again a larger choice will be made available later. If a conservative solution cannot be found we set the solution equal to the high order monotone solution.

# 4 Solid Body rotation tests.

To test the code we perform two test problems for solid body rotation of a given distribution of the scalar on the sphere. These tests are inherently 2-dimensional with no vertical velocity and are usually used as test problems for shallow-water advection schemes. Here we have used a two-level model as this is the lowest vertical resolution we can run the full 3-dimensional code at. However, since the vertical velocity is zero the trajectories should not move off the level they are on and we can thus run the code as two shallow-water models one on top of the other. The results we obtain for each level are the same and so we consider the problems given here as the usual shallow-water advection problems and the solutions we show are those taken from level one of our model.

## 4.1 The Cosine Bell.

This problem is the first one proposed by Williamson et al. [13] for testing shallow-water advection schemes. The initial distribution of the scalar is given by

$$S(\lambda,\phi) = \begin{cases} (S_0/2)(1+cos(\pi r/R)) & \text{if } r < R \\ 0 & \text{if } r \geq R \end{cases} \tag{4.5}$$

where $S_0 = 1000.$, $R = a/3$ and $r$ is the distance form the centre of the cosine bell to the point $(\lambda,\phi)$, with $a = 6371229$ the distance from the centre of the earth to this point in metres. The wind field which provides the solid body rotation is given by

$$u = u_0(cos\phi cos\alpha + sin\phi cos\lambda sin\alpha) \tag{4.6}$$

$$v = -u_0 sin\lambda sin\alpha \tag{4.7}$$

where $u_0 = 2\pi a/(12\text{days})$ gives one complete rotation of the cosine bell in 12 days, and $\alpha$ is an angle in radians relative to the equator at which to send the distribution around the sphere. The test problem is run at $96 \times 73$ resolution with a timestep of 1800 seconds for twelve days with $\alpha = 0, \pi/12, \pi/2$ corresponding to rotation around the equator, at 15 degrees to the equator, and across the poles. This problem has also been attempted with the current Unified Model Eulerian advection scheme, see Malcolm [7] for the results obtained.

The initial data for all the cosine bell tests is shown in figure 1. We first run the $\alpha = 0$ case and to verify our results we compare them with those obtained from the shallow-water model of Bates et al. [1] which uses the departure point method of Robert and cubic Lagrange interpolation. The results for this scheme are shown in figure 2 with the corresponding results for our basic scheme in figure 3. For simplicity we shall refer to our scheme with cubic Lagrange interpolation as the basic scheme, with the monotone cubic Lagrange scheme as the monotone scheme, and with the monotone and conservative scheme as the conservative scheme. The

maximum and minimum values of the two schemes are the same to three decimal places, the results for all the test problems are sumarised in table 4.2. Our scheme shows more noise around the solution, this is rounding error and suggests that the proposed scheme is more susceptible to this than is the scheme of Bates et al. This is not a major concern, since using a minimum contour fractionally bigger than zero would yield cause the two results to look identical.

| Scheme | $\alpha$ | Max Value | Min Value |
|---|---|---|---|
| Basic | 0 | 740.68 | -49.73 |
| Monotone | 0 | 552.34 | 0.00 |
| Basic | $\pi/12$ | 714.40 | -44.58 |
| Monotone | $\pi/12$ | 587.07 | $2.82 \times 10^{-27}$ |
| Basic | $\pi/2$ | 877.78 | -35.82 |
| Monotone | $\pi/2$ | 712.38 | 0.00 |

Table 4.2:

For this test problem, for all values of $\alpha$, it was found that it was impossible to enforce conservation on almost every timestep due to the high order interpolation losing too much of the quantity and there being not enough scope to add it back. Consequently the results for the conservative scheme are not shown as they are identical to the monotone scheme since this is the solution we choose if we cannot enforce conservation. The results for the monotone scheme are shown in figure 4. We can immediately see the lack of any negative values, unlike the basic scheme, and so in this respect the solution is vastly superior. Unfortunately the maximum value of the solution has been reduced markedly and this is a disappointing effect. Bermejo and Staniforth [2] reported that when they implemented a monotone scheme that this *clipping* of the peak did not occur. They used a slightly different specification for the hill, but running this specification rather than the

cosine yielded similar results with the clipping still present. The only differences between the two tests is that theirs was on a uniform square mesh and not on a sphere with the spacings in latitude and longitude different. It appears to be suprising that these details would imply such radically different answers. However, investigation of the code revealed that it was working correctly and that the values obtained by the basic scheme were only so large because it allowed overshoots. The peak value of the basic scheme can be obtained with the monotone scheme if we only constrain the solution to have its minimum value greater than or equal to that of the grid-points around it. This is probably undesirable but may be a fall back position if full monotonicity proves to be too severe a restriction when using real data. This may well be true if we were to try and use the scheme to advect a tracer about, particularly being released from a point source.

The results for the basic scheme for $\alpha = \pi/12$ and $\alpha = \pi/2$ are shown in figures 5 and 7 respectively, with the corresponding results for the monotone scheme in figures 6 and 8. Again we see that the monotone scheme removes the negative values whilst clipping the maximum value. It is interesting to note that the amount of clipping depends on the value of $\alpha$ with the minimum reduction in both absolute and percentage terms being for $\alpha = \pi/12$. We note that the best solution is obtained for advection across the poles, the results for the scheme of Bates et al are identical to those for our basic scheme and so have not been shown. This is because this is the direction with the highest resolution. The worst results, of these 3 cases, were for $\alpha = \pi/12$ demonstrating that the greatest error occurs in moving the field across co-ordinate directions rather than along them.

A feature common to all the solutions, including those obtained with the method of Bates et al, is elongation of the hill in the direction of the flow, with the initial

feature being circular whilst the solutions are all ellipsoids. Since we have used two different departure point methods it suggests that the problem lies with the interpolation scheme. It would be interesting to evaluate other schemes, for example cubic splines, and also other orderings, for example x then y rather than y then x, to see if this problem could be rectified.

## 4.2 The Slotted Cylinder.

This problem is the passive advection of a slotted cylinder, the initial data for which is shown in figure 9, using the same wind fields as used for the previous problem. As all the salient points can be seen from integrating the solution with any one value of $\alpha$, we show the solutions only for $\alpha = 0$. The initial data is given by first defining a cylinder of height $S_0 = 1000$ and radius $R = 15\, a\, \Delta\lambda$ about a point on the equator. A slot $6\, a\, \Delta\phi$ and length $22\, a\, \Delta\lambda$ is then removed from it. The solution from the basic scheme is shown in figure 10 and again exhibits the noise and negative values hich were seen with the first test problem. The maximum value of the solution is 1090.87 and the minimum value is $-68.94$. We now see the overshoots in this problem producing new maxima which was absent from the first test problem. It is again noticable that the solution is elongated in the direction of the flow, as can be seen by looking at the 50 contour. The monotone solution is shown in figure 11 and again demonstrates the successful removal of the negative values, and also does not generate any new maxima. The solution is otherwise very similar to that obtained with the basic scheme and lacks the clipping problem seen with the first example. Figure 12 shows the error in the solution when it is subtracted from the analtic solution. From this picture we can see some noise associated with rounding error and it also easy to see the elongation of the feature in the direction of the flow. We now run the conservative scheme for the same problem. On 64 of the 576 timesteps it was not possible to

enforce conservation, but this is much better than was obtainable with the first test problem. The solution is shown in figure 13 and the error in figure 14. The solution appears to be slighly more noisy than the monotone one, and this is due to rounding error allowing the generation of fractionally bigger values than should be allowed. This supposition can be confirmed by looking at the error picture where this noise appears to have vanished due to rounding error in generating the field to plot. This rounding error problem was of concern in enforcing the minimum value also, but was removed at the cost of an extra *IF* statement in the code at every point in the domain. A similar fix would remove this problem in the maximum calculation.

# 5 Summary and recommendations.

## 5.1 Conclusions and Problems identified.

The departure scheme of McGregor has unacceptably large errors in the local z direction for coarse resolutions and should not be used for such. It is not obvious that it should be used at all in global integrations but should be fine for limited area models.

The scheme gives almost identical results to that of Bates et al for the cosine bell test problem and is thus probably bug free in the horizontal. Tests with idealised data have been performed to check the vertical part of the code.

The monotone scheme performs well for the slotted cylinder problem but suffers from severe clipping of the cosine bell, or if you prefer isolated peak, problem.

The conservative version of the scheme cannot be guaranteed to enforce conservation for any problem, and fails for both these test problems. Although it performs

better for the slotted cylinder problem than the cosine bell problem. This defect is not expected to occur with real data where there is more room for manoeuvre.

All versions of the scheme, and the scheme of Bates et al, suffer from elongation of the feature in the direction of the flow.

## 5.2 recommendations.

1. The departure point scheme of Robert should be coded following Bates et al and used for low-resolution models. The scheme of McGregor should be investigated further in both current climate and operational global model resolutions to see if it should be replaced by the scheme of Robert in these as well. The code will provide a simple switch to choose between them. It is recommended that McGregor's scheme is used with order 4, although this is subject to revision when the scheme is tried with real data.

2. The monotone scheme is susceptible to clipping. Different cubic or higher order interpolants should be coded and evaluated to see if better results can be obtained. It is suggested that cubic spline and monotone cubic Hermite interpolants be coded and evaluated. These schemes will be available along with the cubic Lagrange scheme via a simple switch.

3. The low-order monotone scheme should be the linear Lagrange interpolant. This is because if we want conservation then we need to give the scheme enough of a difference between the low order and high order schemes so that it can find a solution. Alternatively if we went to quintic interpolation for the high order scheme, then it may be possible to get away with a monotone cubic for the low-order scheme.

4. The ability of the conservative scheme to work then using real data should

be monitored. The code will automatically return a warning message if it cannot enforce conservation.

5. The effect of changing the order in which the 1-D interpolants which make up the high order interpolant are done should be investigated. The present choice of y,x,z is computationally the most efficient, but the ordering z,y,x may yield better results.

6. The elongation of the feature in the direction of the flow should be investigated. This may be sensitive to the choice of interpolation scheme and/or the order of the 1-D interpolants which make it up. On the other hand it may be due to a defect common to both departure point schemes.

# Bibliography


[1] J. R. Bates, F. H. M. Semazzi, R. W. Higgins, and S. R. M. Barros. *Integration of the shallow-water equations on the sphere using a vector semi-Lagrangian scheme with a multigrid solver.* Mon. Wea. Rev. **118** pp 1615–1627, 1990.

[2] R. Bermejo and A. Staniforth. *The conversion of semi-Lagrangian advection schemes to quasi-monotone schemes.* Mon. Wea. Rev. **120** pp 2622–2632, 1992.

[3] P. Garcia-Navarro and A. Priestley. *A conservative and shape-preserving semi-Lagrangian method for the solution of the shallow-water equations.* Int. J. Num. Meth. Fluids. **18** pp273–294, 1994.

[4] S. Gravel and A. Staniforth. *A mass conserving semi-Lagrangian scheme for the shallow-water equations.* Mon. Wea. Rev. **122** pp 243–248, 1994.

[5] J. L. McGregor. *Economical determination of departure points for semi-Lagrangian models.* Mon. Wea. Rev. **121** pp 221–230, 1993.

[6] L. M. Leslie and R.J. Purser. *High-order numerics in athree-dimensional time-split semi-Lagrangian forecast model.* Mon. Wea. Rev. **119** pp 1612–1623, 1991.

[7] A. J. Malcolm. *Testing advection schemees for the shallow-water equations on a set of test problems. I* F. R. Division Tech. Note No 83, 1994.

[8] M. H. Mawson. *The proposed semi-Lagrangian advection scheme for the semi-implicit Unified Model integration scheme.* F. R. Division working paper No 162, 1994.

[9] A. Priestley. *A quasi-conservative version of the semi-Lagrangian advection scheme.* Mon. Wea. Rev. **121** pp 621–629, 1993.

[10] A. Robert. *A stable numerical integration scheme for the primitive meteorological equations.* Atmos. Ocean. **19** pp 35–46, 1981.

[11] A. Staniforth and J. Côté. *Semi-Lagrangian integration schemes for atmospheric models - A review.* Mon. Wea. Rev. **119** pp 2206–2223, 1991.

[12] D. L. Williamson and P. J. Rasch. *Two-dimensional transport with shape-preserving interpolation.* Mon. Wea. Rev. **117** pp 102–129 1989.

[13] D. L. Williamson, J. B. Drake, J. J. Hack, R. Jakob, and P. N. Swarztrauber. *A standard test set for numerical approximations to the shallow-water equations on the sphere.* J. Comp. Phys. **102**, pp211–224, 1992.

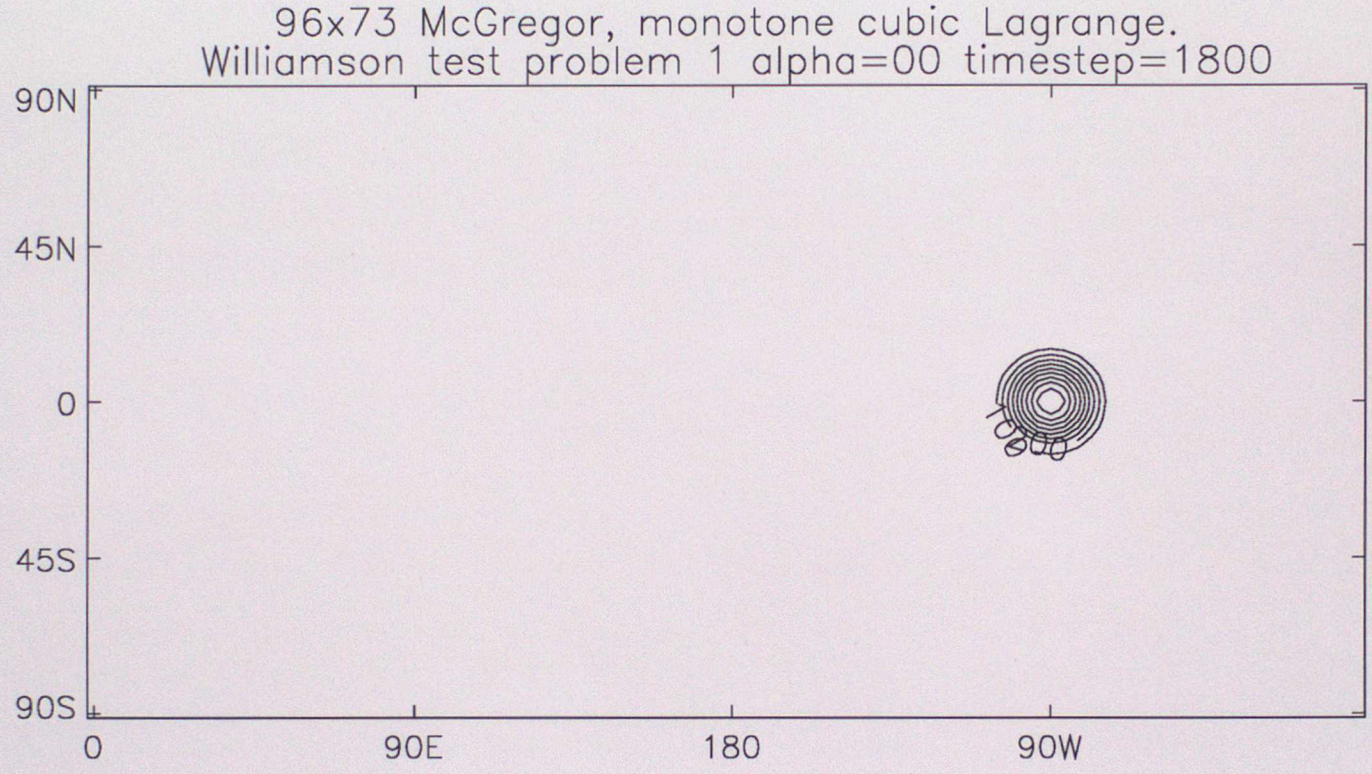


Figure 1: Initial field.

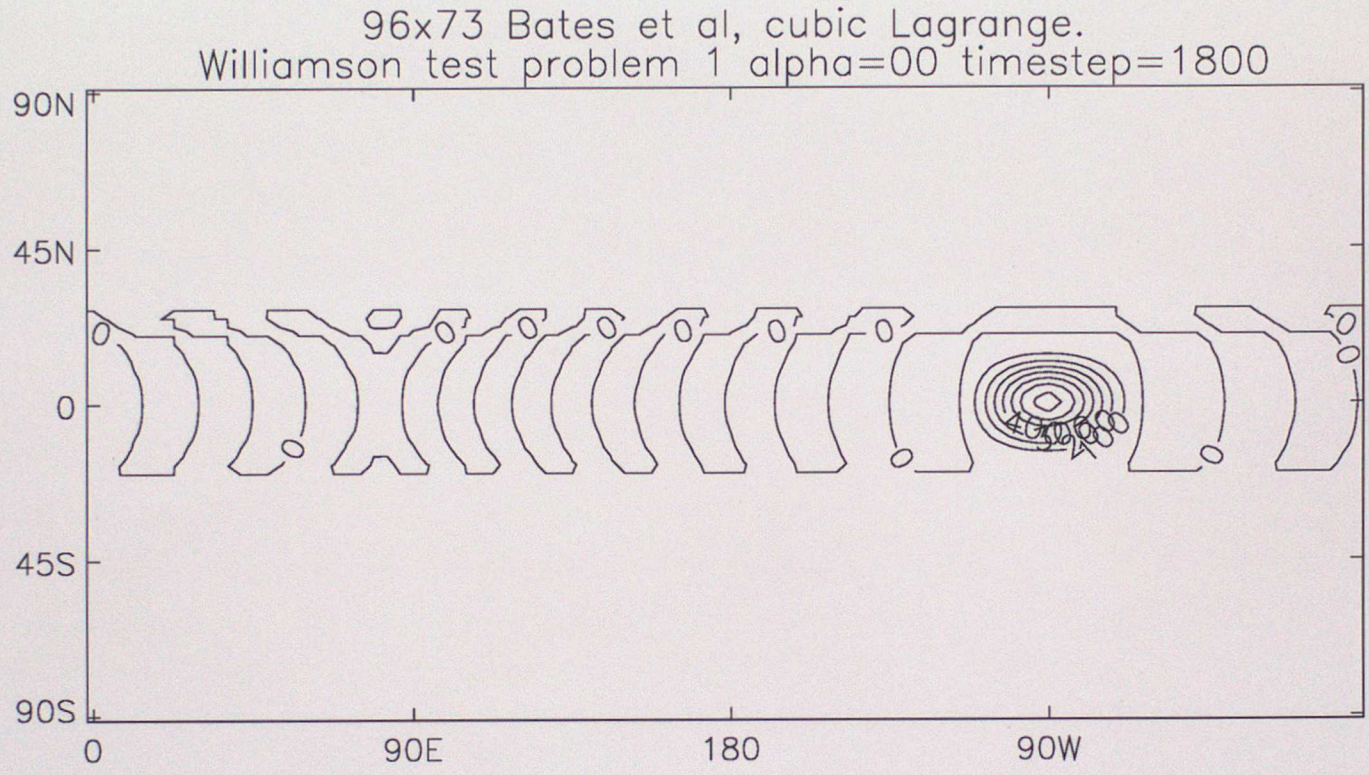


Figure 2: Field after one revolution.

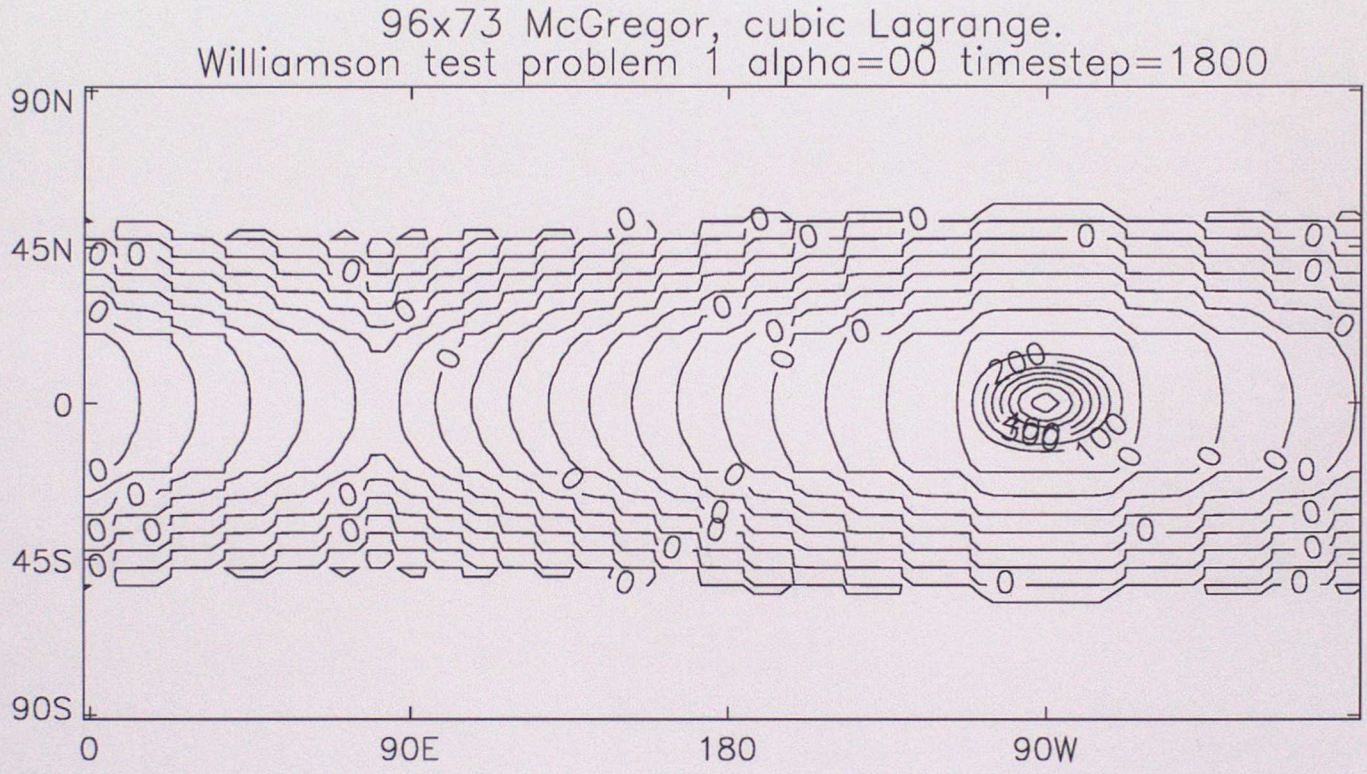


Figure 3: Field after one revolution.

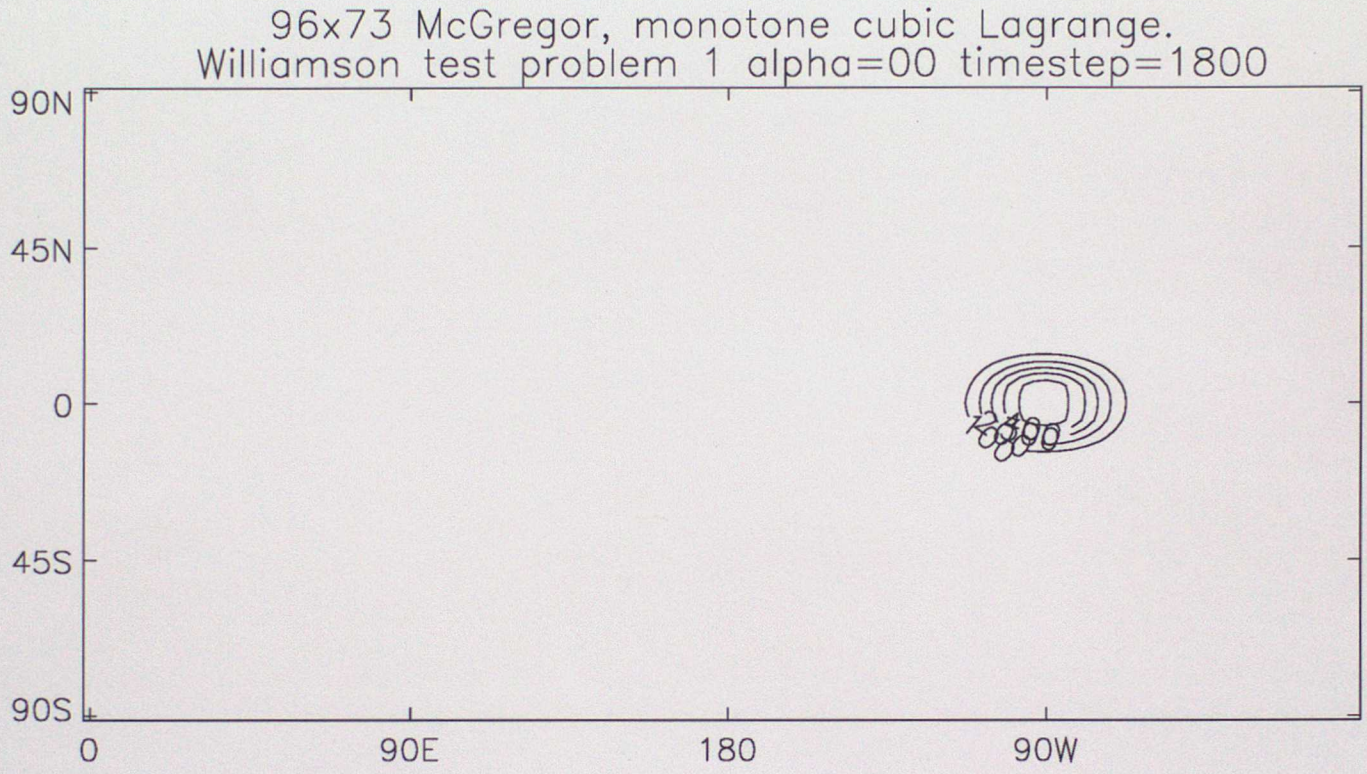


Figure 4: Field after one revolution.

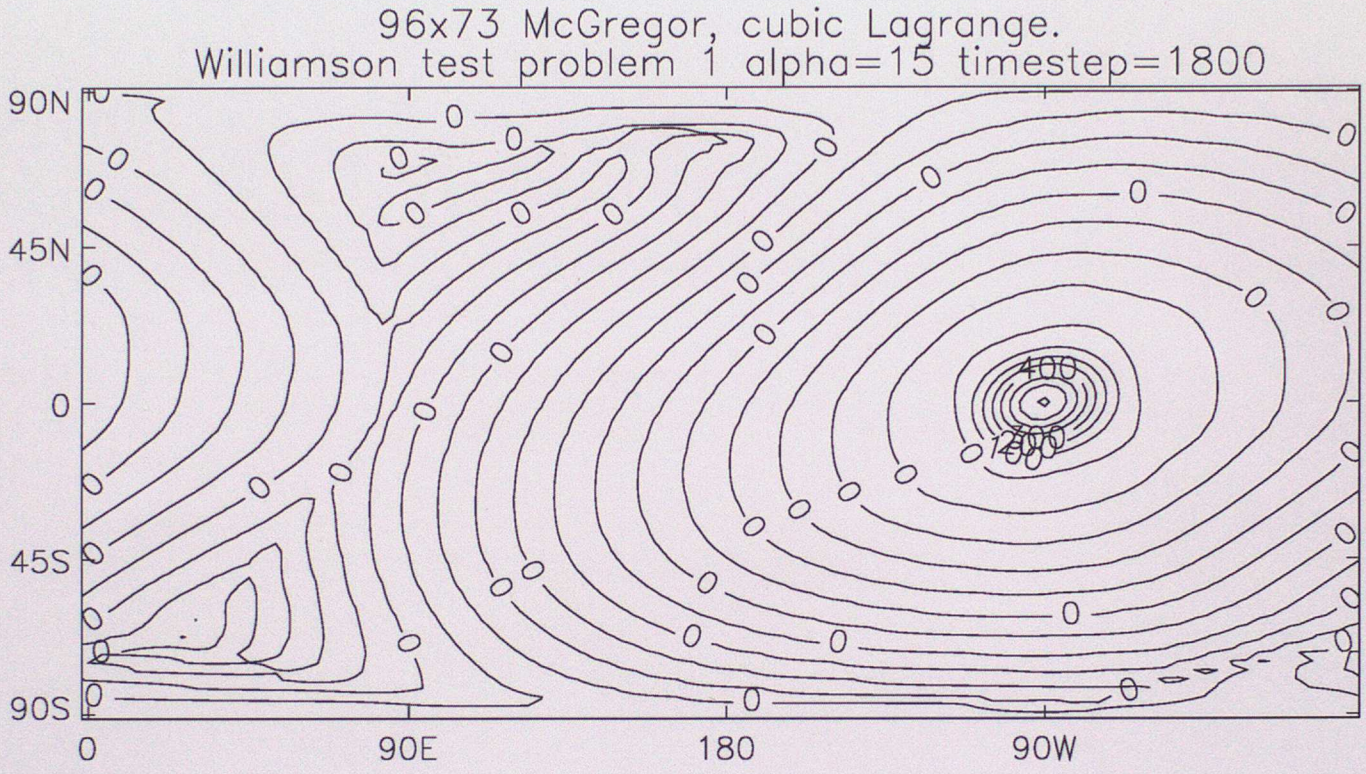


Figure 5: Field after one revolution.

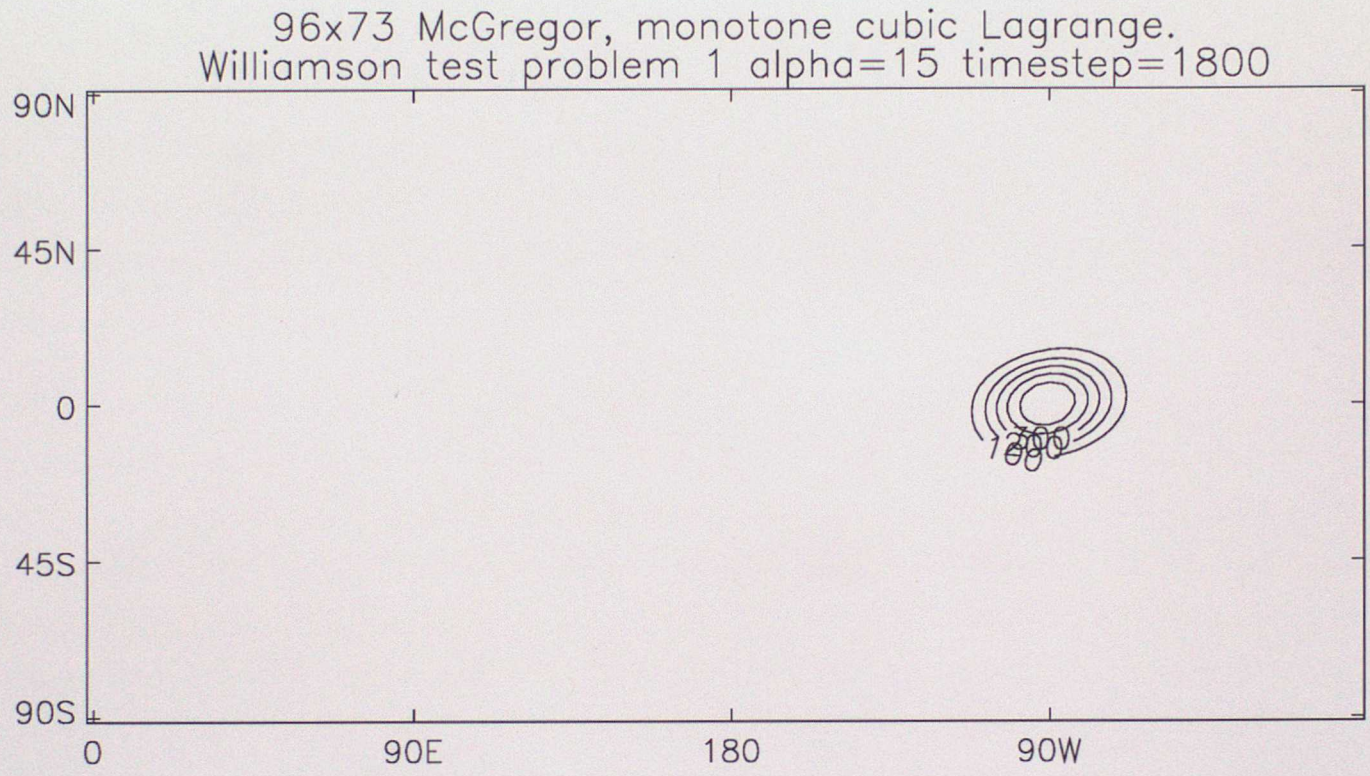


Figure 6: Field after one revolution.

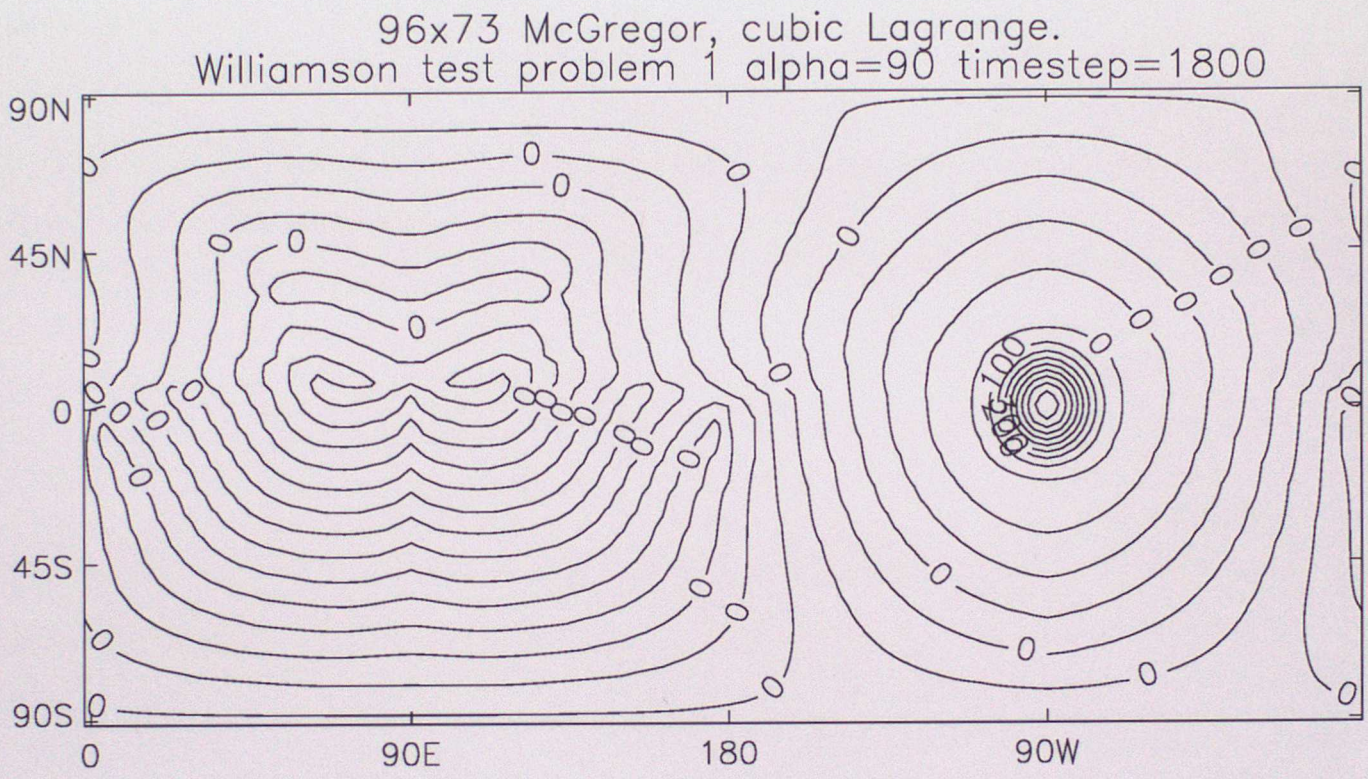


Figure 7: Field after one revolution.

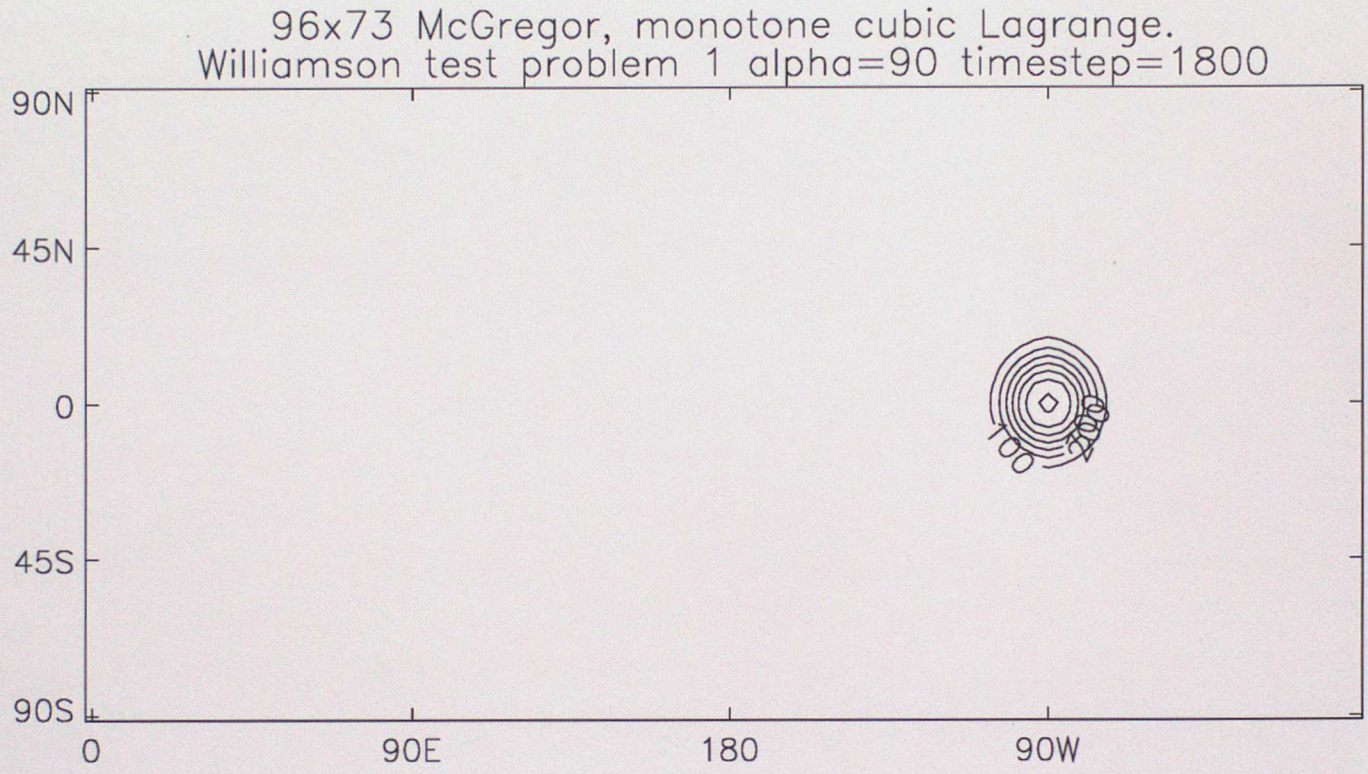


Figure 8: Field after one revolution.

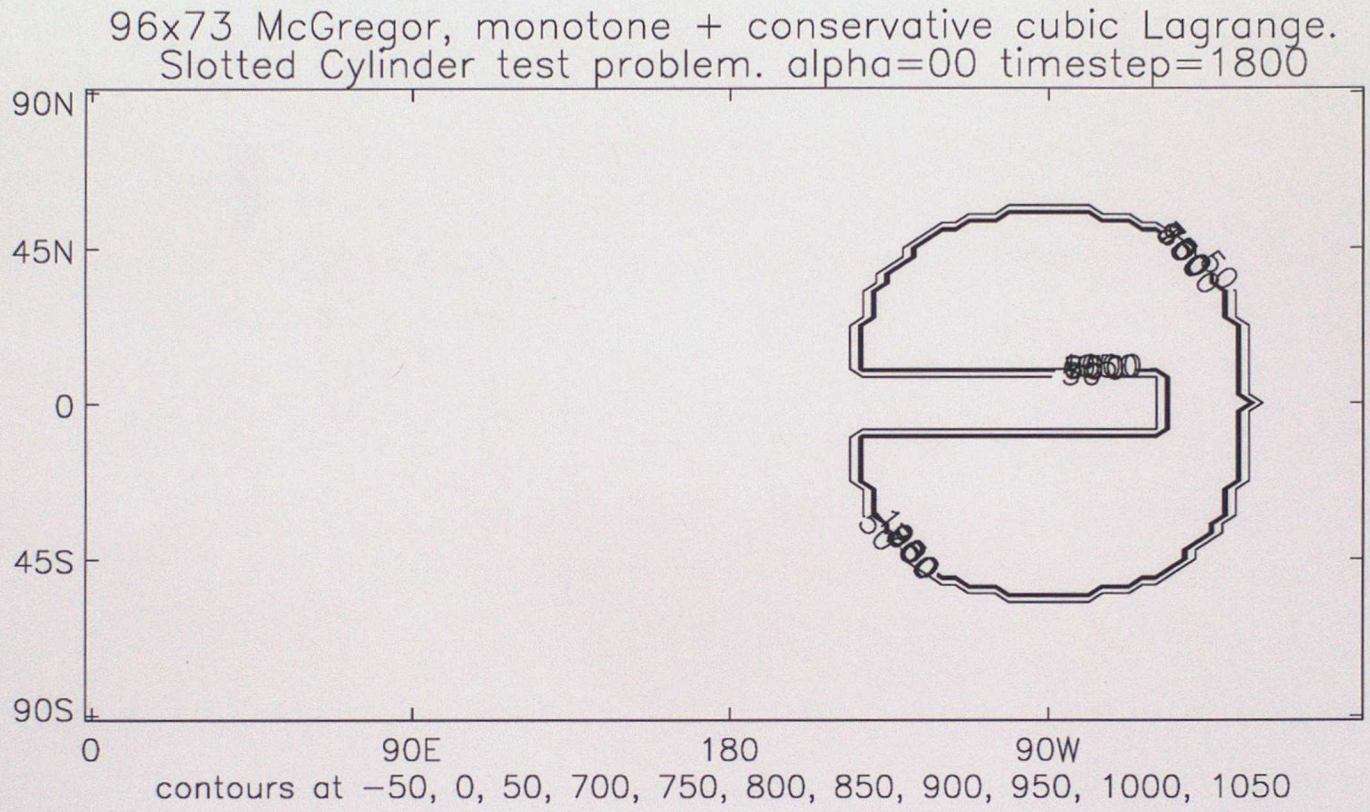


Figure 9: Initial field.

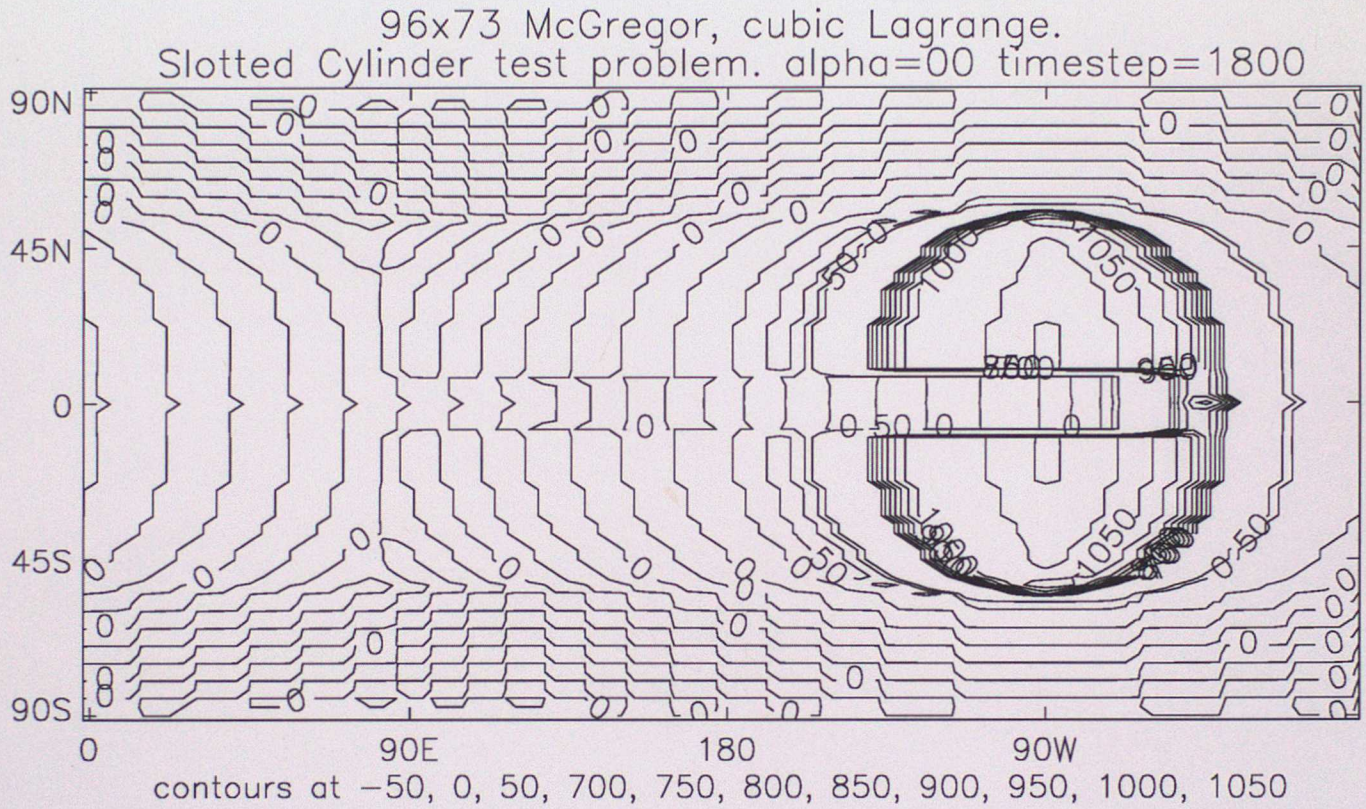


Figure 10: Field after one revolution.

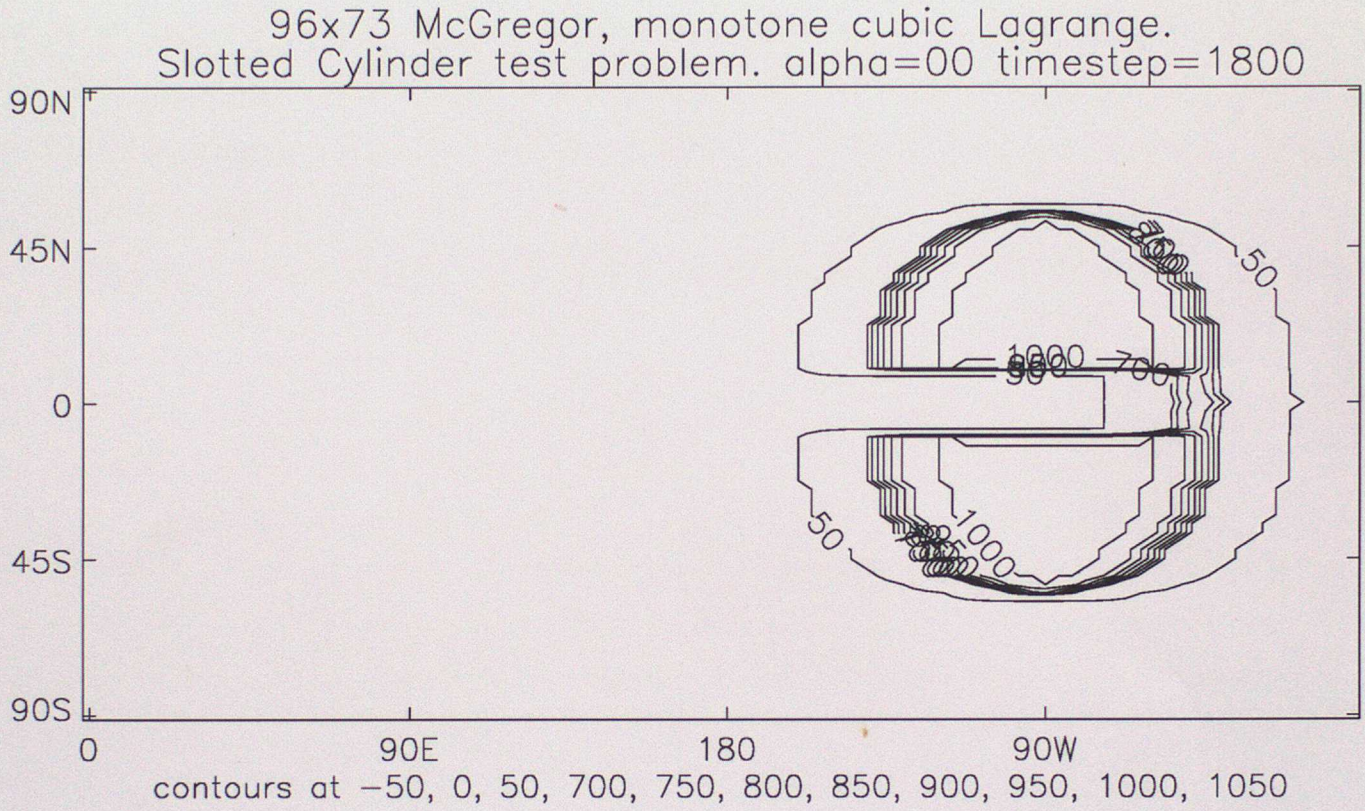


Figure 11: Field after one revolution.

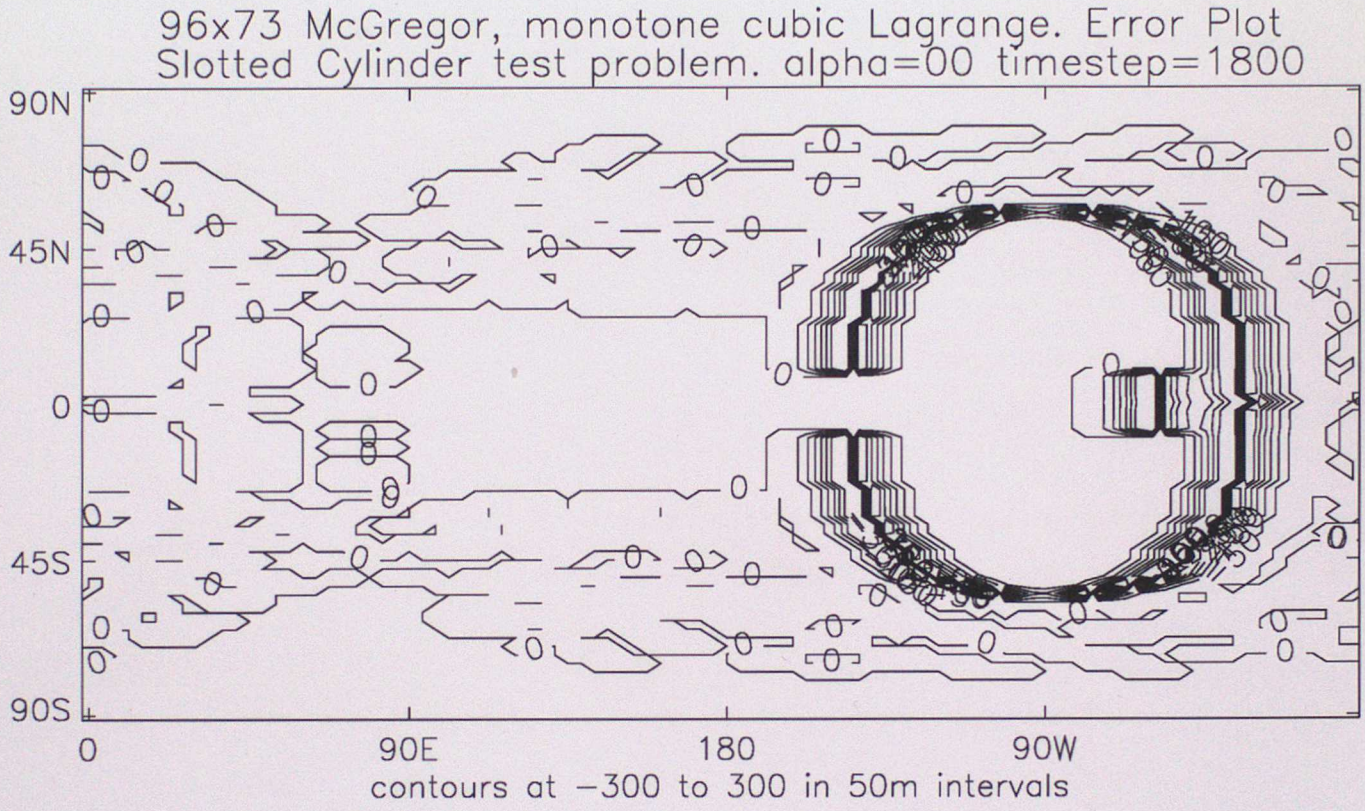


Figure 12: After one revolution.

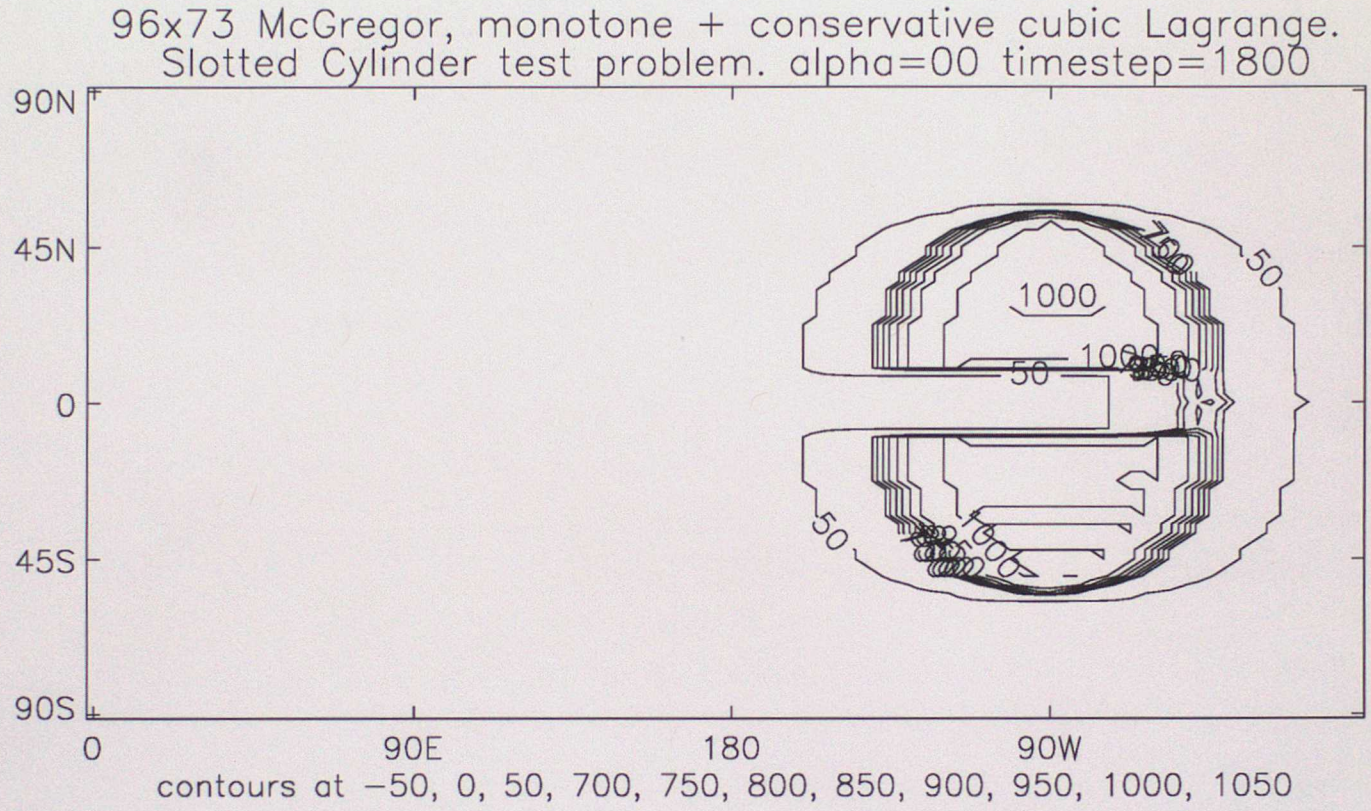


Figure 13: Field after one revolution.

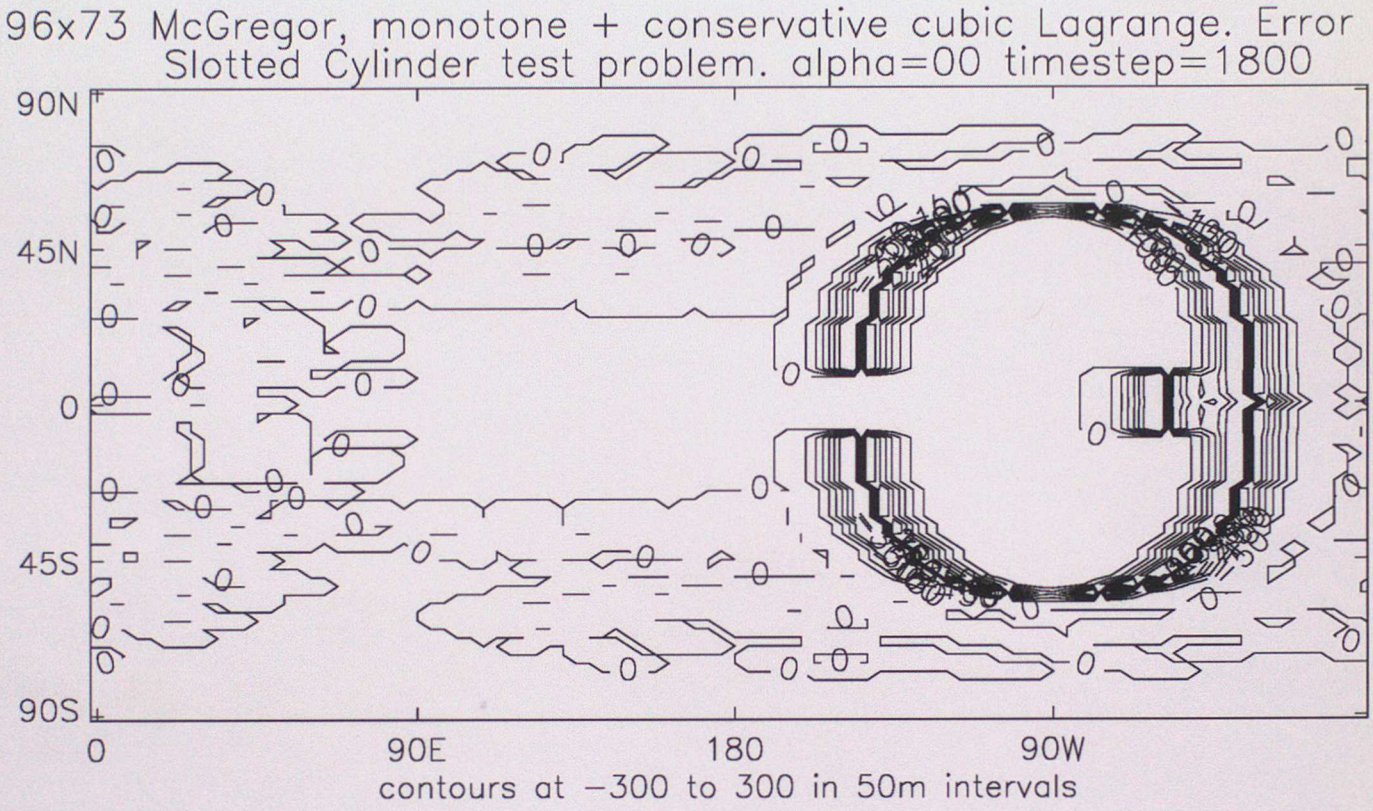


Figure 14: After one revolution.